

CONCEPTUAL DESIGN OF 100 MeV SEPARATED SECTOR CYCLOTRON

B. Mahdian, H. Afarideh*, R. SolhjousMasouleh, Department of Energy Engineering & Physics, Amirkabir University of Technology, Tehran, 15875-4413, Iran

M. Ghergherehchi, J. S. Chai, WCU Department of Energy Science/School of Information & Communication Engineering, Sungkyunkwan University, Suwon 440-746, Korea

Abstract

The 100 MeV separated sector cyclotron, aimed for various applications including radioactive ion-beam (RIB) production and proton therapy, was designed at Amirkabir University of Technology (AUT). It has four separated sector magnets. The cyclotron magnet design was based on an iterative process starting from a simple model requiring the vision of the complete cyclotron and the possibility of integration of all subsystems. By computer simulation with the 3D (CST) and 2D (POSSION) codes, principle parameters of the cyclotron magnet system were estimated (pole radius 180 cm, outer diameter 640 cm, height 300 cm). The results showed that the isochronous deviations between simulated values and the calculation one are smaller than 5 Gauss at most radii; therefore, it fulfilled the requirements. This work has been done with high accuracy, proved by particle trajectories and considered mesh range. It has been concluded that it can be possible to design and develop this high energy cyclotron by introducing simple model without using trim and harmonic coils.

INTRODUCTION

Due to the increasing need for accelerators in various research fields such as nuclear physics, atomic physics, material science, biology, and medical science, Amirkabir University of Technology (AUT) has aimed to design isochronous cyclotrons. One of the applications of cyclotrons these research fields are interested in is producing radioactive ion-beam (RIB), can be obtained by a 100 MeV separated sector cyclotron. Magnet, designed based on an iterative process, is considered as one of the most important parts of cyclotron. Two main goals were satisfied in this paper; first, obtaining an average field, rising appropriately with radius, and then, maintaining orbit stability. The main parameters of the magnet will be presented in Table 1. The whole structure of the designed magnet is shown in Fig. 1.

BASIC CONSIDERATIONS

Because of the fact that small gap between poles reduces the number of ampere-turns, necessary to produce the required magnetic field [1], 3 cm pole gap was selected. Four-fold configuration was adopted not only to avoid the effects of the resonances like and [2] but also to increase the acceptable maximum energy [3].

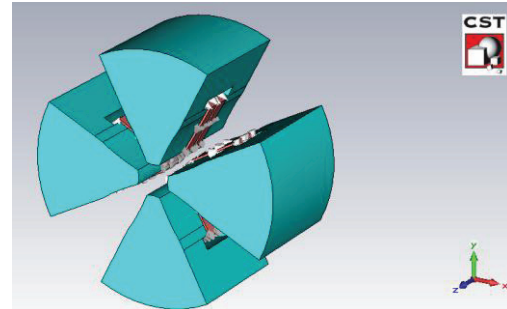


Figure 1: Whole structure of the magnet.

Table 1: Main Magnet Parameters

Parameters	Values
Pole radius	180 cm
Height	300 cm
Sector angle	46-54 degree
Sector Gap	3 cm
Number of sectors	4

MAGNET MODEL CORRECTION

The hard-edge magnet model was used to give an approximate solution to convert magnetic field error to corresponding sector angle error, as shown in Eq. (1),

$$\Delta\eta(r) = \Delta B(r) \cdot \frac{2\pi/N}{B_{hill}(r) - B_{valley}(r)} \quad (1)$$

Usually, $\Delta\eta(r)$ used for model correction needs to be multiplied with a scaling factor σ with the value between 0.5 ~ 0.9 to avoid oscillation of field error during iteration [4]. Shimming process was followed as an iterative process until the magnetic field error along radius become minimum value. All the diagrams and error calculations were obtained using MATLAB program.

HAND CALCULATIONS

Prior to 3D simulation with CST code [5], basic dimensions of the magnet had been calculated. Under consideration of magnetic rigidity, calculated according to the following equation, extraction radius and maximum magnetic field on the hill regions were figured out respectively 148.7 cm and 1.7 Tesla. Based on the ampere law, the number of ampere-turns was estimated to be 26.4 kA*turns.

*corresponding author: hafarideh@aut.ac.ir

$$\langle B \rangle . R = \sqrt{T^2 + 2.T.E_0} / 300.Z \quad (2)$$

After having done hand calculations, 2D simulation was carried out to prove the results of obtained basic dimensions. In order to meet this, Poisson 2D code, having the advantage of using small mesh size for areas with high magnetic field gradient [6], was used. Figure 2 presents the 2D field distribution on the symmetry plan in the hill.

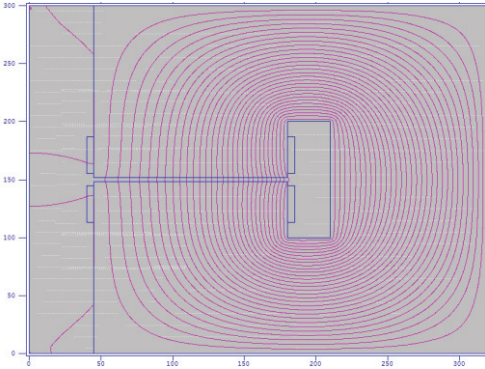


Figure 2: 2d simulation with Poisson code.

MAGNETIC FIELD OPTIMIZATION

After having considered all aspects above, iterative process was started in order to optimize the magnetic field. The theoretical equation for fulfilling this is:

$$\langle B \rangle = \frac{2.\pi.f.m_0}{h.q} \cdot \sqrt{1 - 4.\pi^2.R^2.f^2 / h^2.c^2} \quad (3)$$

The aim of iterative process is to make $\Delta B = \langle B \rangle - \langle B_c \rangle$ to approach zero as much as possible (The calculation value $\langle B_c \rangle$ was calculated by CST software) [7]. Averaged magnetic field diagram was shown in Fig. 3.

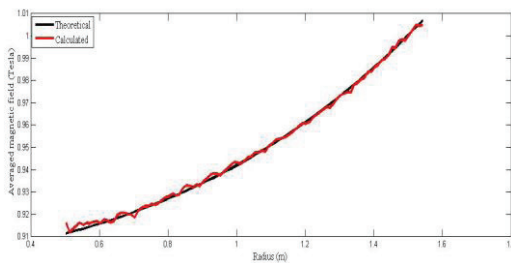


Figure 3: Averaged magnetic field.

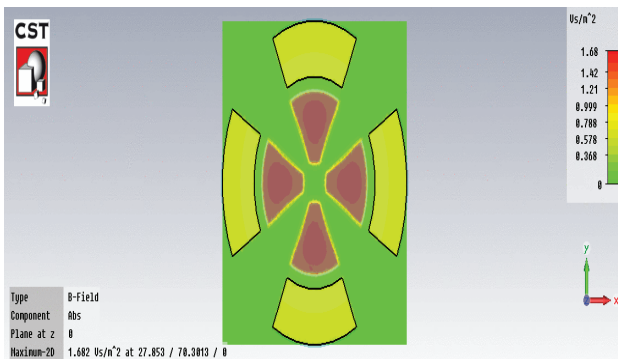


Figure 4: Field distribution in mid-plane.

Figure 4 illustrates that the maximum magnetic field in the mid-plan is far away from the saturation point of the used material (steel 1010). It is beyond the dispute that the precision of the simulation depends on the selected mesh range very much, so a logical mesh number was selected according to the sweeping the magnetic field on extraction radius with the mesh number. Figure 5 illustrates that the increase in the mesh number (mesh parameter) leads to the approximately constant averaged magnetic field on extraction radius after the mesh number=40.

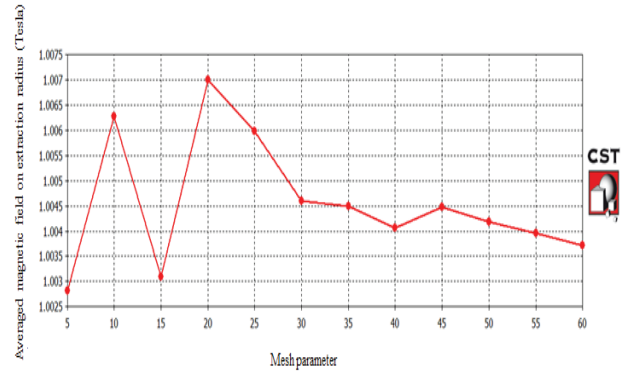


Figure 5: Averaged magnetic field on extraction radius versus mesh number in the volume of the magnet.

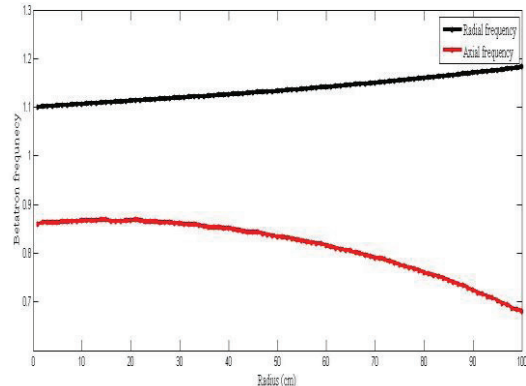


Figure 6: Radial and Axial frequencies.

PARTICLE DYNAMIC ANALYSIS

The results of the radial and vertical frequencies have been shown in Fig. 6. Resonance diagram for all resonances up to 3rd order with $|k| + |l| \leq 3$ were sketched in Fig. 7 [8]. Dangerous resonances like integer ($\nu_z = 1, \nu_r = 1$), and half integer ($\nu_z = 1/2, \nu_r = 3/2$) were avoided [9]. The results confirmed that the working points are far from dangerous resonance zones. The beam tracking simulation has been done by CST particle studio [5]. In this simulation, space charge was not considered and only beam trajectories on the middle of the hill gap were plotted. The trajectories of beam from 10 MeV to 100 MeV have been plotted in Fig. 8 with 10 MeV increment. It depicts clearly the proper beam trajectories on the mid-gap on the hill.

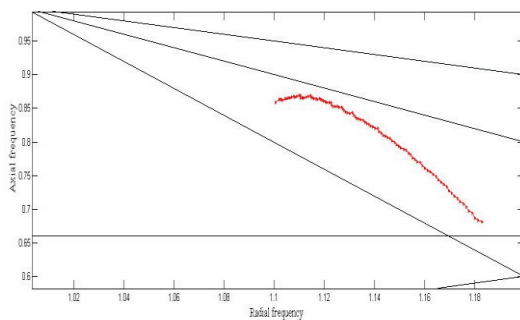
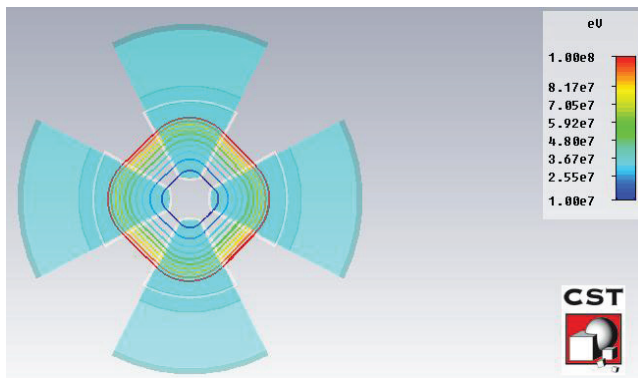
Figure 7: Resonance diagram up to 3rd order.

Figure 8: Particle trajectories.

CONCLUSION

The design and simulation of the 100 MeV separated sector cyclotron magnet has been carried out with high accuracy and without trim and harmonic coils. The maximum deviation between calculated values and theory is about 35 Gauss. The tune diagram shows that the working points are far away from all resonances up to 3rd order. The trajectories of beam from 10 MeV to 100 MeV show the proper beam trajectories on the mid-gap on the hill.

REFERENCES

- [1] S. Zarembo, Magnet for cyclotrons, CERN-2006-012, (2006).
- [2] K.M.H. Gad et al., "Magnet design of 70 MeV Separated Sector Cyclotron," MOPCP033, Proceedings of CYCLOTRONS 2010, Lanzhou, China.
- [3] John J. Livingood, *Principles of Cyclic Particle Accelerators* (D. Van Nostorand, 1961).
- [4] B. Qin et al., Nucl. Instr. and Meth. in Phys. Research A. 620, 121 (2010) 127.
- [5] CST EM and Particle studio manual, (2011).
- [6] User's guide for the POISSON/SUPERFISH Group of Codes, LA-UR-87-115, Los Alamos Accelerator Code Group.
- [7] Q.G. Yao et al., "The Isochronous Magnetic Field Optimization of HITFIL Cyclotron", MOPCP002, Proceedings of Cyclotron 2010, Lanzhou, China.
- [8] Helmut. Wiedemann, *Particle Accelerator Physics*, (Springer Berlin Heidelberg New York, 2007).
- [9] S.Y. Lee, *Accelerator physics*, (World Scientific Co. Pte. Ltd, 2004).